Korean J. Chem. Eng., **27**(2), 658-665 (2010)
DOI: 10.1007/s11814-010-0097-7

Rheological property and curing behavior of poly(amide-*co*-imide)/multi-walled carbon nanotube composites

Seung Hwan Lee*, Sheong Hyun Choi, Jin Il Choi***, Jae Rock Lee***, and Jae Ryoun Youn*,†**

*Research Institute of Advanced Materials (RIAM), Department of Materials Science and Engineering, Seoul National University, Seoul 151-744, Korea
**The Technology Commercialization Center, Hyosung Corporation, Anyang-si, Gyeonggi-do 431-080, Korea
***Advanced Materials Division, Korea Research Institute of Chemical Technology, P.O. Box 107, Yuseong, Daejeon 305-600, Korea
(*Received 16 June 2009 • accepted 15 October 2009*)

Abstract−Poly(amide-*co*-imide) (PAI)/multi-walled carbon nanotube (MWCNTs) composites were prepared by using solution mixing with ultrasonication excitation in order to investigate effects of MWCNTs on rheological properties and thermal curing behavior. Steady shear viscosity of the composite showed bell shaped curves with three characteristic patterns: shear thickening, shear thinning, and Newtonian plateau behavior. Both storage modulus and complex viscosity were increased due to higher molecular interaction than that of the pure PAI resin. Especially, hydrogen peroxide treated MWCNT/PAI composites had the highest storage modulus and complex viscosity. Glass transition temperature of the PAI/MWCNT composite was increased with increasing MWCNT content and thermal curing time since the mobility of PAI molecules was reduced as more constraints were generated in PAI molecular chains. It was found that thermal curing conditions of PAI/MWCNT composites are determined by considering effects of weight fraction and surface modification of MWCNTs on internal structure and thermal properties.

Key words: Poly(amide-*co*-imide), MWCNTs, Rheology, Glass Transition Temperature, Thermal Curing

INTRODUCTION

Thermoplastic poly(amide-*co*-imide), PAI, is one of the high performance engineering plastics which have outstanding mechanical properties, low thermal expansion coefficient, and excellent thermal stability. It has been widely used for wear resistant devices, electrical insulating wires, filtration media, and reinforcements by using superior physical and chemical properties, e.g., stability against strong acids and most organics at high temperature. It is also well known that the PAI resin has synergetic properties due to characteristics of both polyamides and polyimides existing in the molecular backbone. Furthermore, PAI resin is a promising candidate as the matrix material for hybrid composites since carboxyl groups can induce hydrogen and ionic bonding. However, PAI resin should be converted into the final form through imidization with thermal and chemical routes. To stabilize the internal structure and improve physical properties, post-treatments such as heat treatment, curing, imidization, or carbonization are needed at high temperature [1-5].

Carbon nanotubes, CNTs, have outstanding mechanical, electrical, and thermal properties due to their high aspect ratio and unique arrangement of carbon hexagons in tube-like fullerenes. When high performance properties are required for special applications, they have been employed by incorporating CNTs into various matrices. Especially, polymer/CNT composites have attracted great interest owing to their unique mechanical and multi-functional properties resulting from the high aspect ratio and large surface area of CNTs. However, they tend to be entangled together leading to many defects in composites and low efficiency of CNTs in polymer matrices [6-10]. Dispersion of CNTs is an important factor for physical properties of polymer/CNT composites. Nowadays, one of the main issues on polymer/CNT composites is how to improve the dispersion of CNTs in a polymer matrix [11-14]. To improve the dispersion of CNTs in polymer matrix, two types of bonding method, covalent and non-covalent, have been applied through chemical modification or wrapping of the CNT surface, respectively. Chemical modification methods such as acid, fluorine, hydrogen peroxide treatment, have been applied to generate useful functional groups that can induce strong interaction with matrix polymers.

Recently, many studies for PAI composites filled with nanofillers have been conducted to improve physical properties and wear resistance of the pure resin. However, there were few studies about PAI/MWCNT composites since PAI has high glass transition temperature (T_g) and a long time is needed for sufficient imidization at high temperature [15-19]. Rheological properties are investigated in order to understand internal structure and processability of polymer/CNT composites since they can reflect various physical properties of polymer composites. Information on three-dimensional network structure formed by reinforcing fillers, dispersion state of fillers, and degree of interaction between fillers and polymer matrix can be obtained from measurement of the rheological properties [20-22]. In this study, functionalized MWCNT/PAI composites were prepared by solution mixing with ultrasonic excitation. Then, effects of sur-

†To whom correspondence should be addressed.
E-mail: jaeryoun@snu.ac.kr
‡This paper is dedicated to Professor Jae Chun Hyun for celebrating his retirement from Department of Chemical and Biological Engineering of Korea University.

face functionalization and amount of MWCNTs on rheological properties of PAI/MWCNT suspensions were investigated at steady and dynamic oscillatory shear flows. Finally, thermal curing behavior of pure PAI and PAI/MWCNT composites was analyzed through T_g analysis obtained from differential scanning calorimeter (DSC) measurements.

EXPERIMENTAL

1. Materials

Poly(amide-*co*-imide) resin (Torlon®4000T-HV, Solvay Advanced Polymers, U.S.A) was used as the matrix in this study. It was supplied as crude PAI powders, and its chemical structure and NMR spectrum are shown in Figs. 1(a) and (b), respectively. It was made from trimellitic anhydride chloride and a mixture of aromatic diamines. It also contains amide and imide groups in the molecular backbone, but one resin has ether linkages in diamine components and the other did not. Intrinsic viscosity range was 0.70-0.90 (0.5 wt% NMP at 25 °C) and the particle size ranges from 30 to 40 μm [3,23]. To confirm the degree of imidization for the PAI resin and to compare with chemical structure reported to recent reference [3], NMR analysis was performed with NMR spectrometer (Bruker AMX-

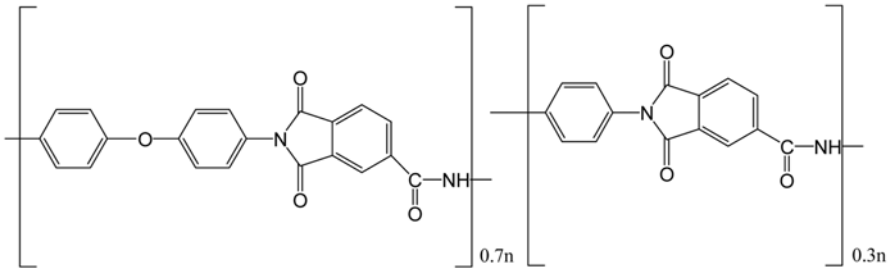

(a)

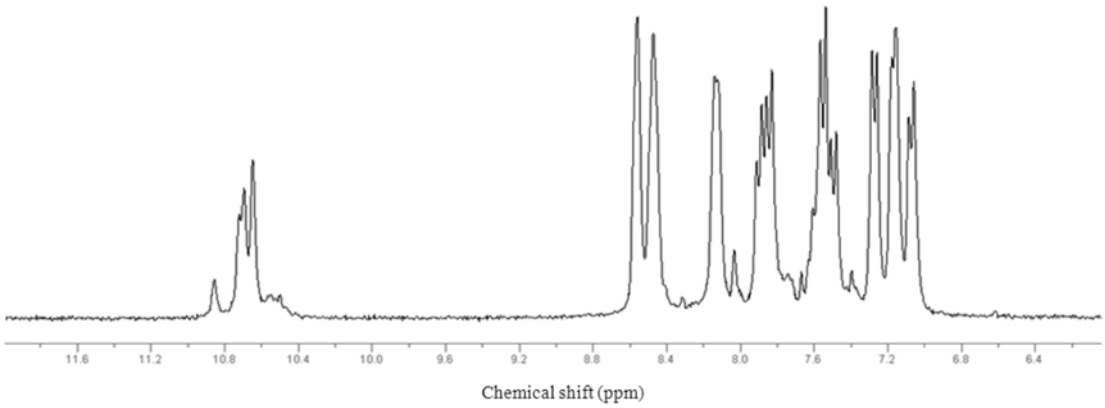

(b)

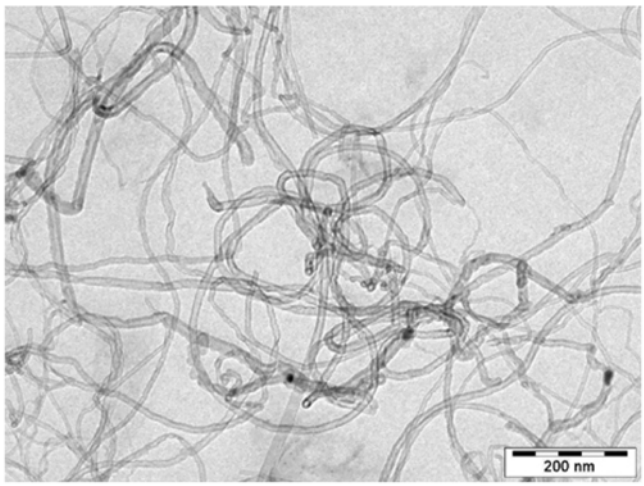

(c)

Fig. 1. (a) Chemical structure of Torlon® poly(amide-*co*-imide), (b) NMR spectrum of as-received PAI powders, and (c) TEM picture of pristine MWCNTs used in this study.

Table 1. Composition of pure PAI and PAI/MWCNT composite films prepared with solution mixing and film casting (wt%)

	Pristine MWCNTs	a-MWCNTs	h-MWCNTs	p-MWCNT
Pure PAI				
PAI/MWCNT1.0	1.0			
PAI/a-MWCNT1.0		1.0		
PAI/h-MWCNT1.0			1.0	
PAI/p-MWCNT0.5				0.5
PAI/p-MWCNT1.0				1.0
PAI/p-MWCNT1.5				1.5
PAI/p-MWCNT2.0				2.0

500-FT, U.S.A) after dissolving PAI powders with dimethylsulfoxide solvent at room temperature to prevent additional cyclization reaction. MWCNTs (Carbon Nano-material Technology, Pohang, KOREA) were produced by the catalytic chemical vapor deposition method. As shown in Fig. 1(c), the diameter of MWCNTs ranged from 5 to 20 nm; the length is larger than 10 μm, and therefore the aspect ratio was higher than five hundred. Specific surface area of the MWCNT measured by using the BET method ranged from 100 to 700 m^2/g and bulk density was in the range of 0.08-0.12 g/cm^3 [24]. *N*-methyl-2-pyrrolidone (NMP, Daejung Chemicals & Metals, KOREA) was used as the solvent to dissolve crude PAI powders.

2. Chemical Modification of MWCNTs

Chemical functionalization of the MWCNT surface was performed with three methods: acid, hot air, and hydrogen peroxide treatments. Pristine MWCNTs were acid treated by dispersing the MWCNTs in a 65% solution of 3 : 1 mixture of H_2SO_4/HNO_3 in water. Then, the suspension was treated by ultrasonic excitation at 80 °C for 1 hour in order to attach carboxyl and hydroxyl groups onto the surface of MWCNTs. After the acid treatment, the MWCNTs were cleaned several times with distilled water, filtered by using filtering paper, and then dried at 50 °C in vacuum oven for 2 days. Hydrogen peroxide treated MWCNTs (p-MWCNTs) were obtained through similar method to the acid treatment. Pristine MWCNTs were dispersed in the 1 : 1 mixture of H_2O_2/distilled water. Then, the mixture was sonicated at 80 °C for 1 hour. After the hydrogen peroxide treatment, the mixture was cleaned several times with distilled water and was filtered by using a filtering paper. p-MWCNTs were dried in a vacuum oven at 50 °C for 2 days. Heat treated MWCNTs (h-MWCNTs) were also obtained by heating MWCNTs at 500 °C for 1 hour in a furnace with air circulation.

3. Preparation of PAI/MWCNT Composite Films

PAI/MWCNT composites were prepared by mechanical mixing of MWCNTs under ultrasonic excitation, film casting, and thermal curing processes. Three types of surface modified MWCNTs were dispersed in NMP for 1 hour under ultrasonic excitation at room temperature. After MWCNTs were dispersed in the solvent sufficiently, the crude PAI resin was added into MWCNT/NMP suspension. To make perfect PAI/MWCNT/NMP solution, the solution was mixed by using a mechanical agitator at 100 °C for 1 day. Finally, the suspension was sonicated for 2 hours to obtain good dispersion of MWCNTs in PAI/NMP solution. By using the solution mixing process, four kinds of PAI/NMP solutions, 10, 15, 20 and 25 wt%, were prepared. PAI concentration of 15 wt% was determined for successful film casting after the solutions were cast and the films were evaluated. Weight fraction of the MWCNTs in the PAI/MWCNT composite was chosen to be 0.5, 1.0, 1.5 and 2.0 wt% as shown in Table 1.

Table 2. Thermal curing conditions used for pure PAI and PAI/MWCNT composite films

Total curing time	Preheating time (min)	Raising time (min)	Holding time (min)
Without curing	-	-	-
6 hrs	10	145	205
9 hrs	10	220	310
12 hrs	10	295	415
18 hrs	10	440	630

After PAI/MWCNT suspensions with different concentrations were prepared, they were poured into a rectangular mold surrounded by Teflon film. They were dried in a convection oven at 80 °C for 2 days to remove the solvent and additional drying was conducted in a vacuum oven at 40 °C for 3 days. Since thickness of the cast specimen was not uniform, compression molding was additionally performed at 150 °C for 15 minutes under 15 tons by using a hot press (WABASH METAL PRODUCTS, U.S.A). Thickness of the PAI/MWCNT composite film was about 400 μm. To convert the crude PAI into the final product, the PAI resin must be cured thermally with different time sequences. The PAI/MWCNT composite film was thermally cured in a furnace (L15/1100/P320, NABERTHERM, GERMANY) with air circulation. As listed in Table 2, curing time consisted of three steps: pre-heating, raising, and holding steps. Pre-heating was carried out for 15 minutes, and raising and holding steps were maintained with the time ratio of 7 : 10. Five specimens were prepared through different thermal curing steps with the total curing time of 0, 6, 9, 12, and 18 hours.

4. Characterization

Functional groups generated on the MWCNT surface were detected between 650 to 4,000 cm^{-1} by Fourier transform infrared spectroscopy (FT-IR, JASCO 660 Plus, JASCO, JAPAN) using a potassium bromide reference. Rheological properties of the pure PAI and PAI/MWCNT solutions were investigated by using a rotational rheometer (AR2000, TA Instruments, U.S.A). The measurement was conducted by using corn and plate geometry (corn angle=2°) with the diameter of 40 mm and 53 μm truncation gap at room temperature. Steady shear flow was used for rheology measurement at the shear rate ranging from 0.001 to 10 s^{-1}. Dynamic oscillation shear

flow was investigated at the angular frequency ranging from 0.1 to 100 rad/s with the constant strain of 3.0% in order to measure linear viscoelastic behavior of the sample. The DSC data was obtained with a Perkin-Elmer DSC 6 instrument, which operated in the power compensation mode. The system was calibrated using elemental indium and 6.5±1.0 mg of the sample was used for each run. The first heating run was performed from 30 ºC to 400 ºC at the heating rate of 20 ºC/min. The sample was held at 400 ºC for 5 minutes and then cooled to 30 ºC at a cooling rate of 20 ºC/min. The second scan was run from 30 ºC to 400 ºC at the heating rate of 20 ºC/min, and the glass transition temperature was measured from the second heating curve.

RESULTS AND DISCUSSION

1. Chemical Structure of Surface Treated MWCNTs

It is possible to identify functional groups from characteristic position, width, and intensity of their FI-IR spectra. As shown in Fig. 2, a-MWCNTs show some other peak bands in contrast with the spectrum of untreated MWCNTs. The broad peak around 3,438 cm^{-1} is assigned to hydroxyl (O-H) groups, and the peak around 1,634 cm^{-1} is assigned to carbonyl (C=O) groups, and the very weak peak around 1,072 cm^{-1} is assigned to carbon - oxygen single bond (C-O). These results show that the hydroxyl and carbonyl groups were attached to the surface of MWCNTs by the acid treatment [9, 10,13]. In the case of h-MWCNTs, the spectrum pattern was similar to that of a-MWCNTs, but the intensity of each peak was increased slightly when compared with a-MWCNTs. Oxidation reaction onto MWCNT surface had occurred during heat treatment in hot air of 500 ºC. In the case of p-MWCNTs, a characteristic band was observed at around 1,089 cm^{-1}. This peak was much stronger than peaks of MWCNTs treated with acid or hot air, which indicates that many C-O single bonds were generated onto the surface of MWCNTs during hydrogen peroxide treatment [10]. Therefore, it is concluded that hydrogen peroxide treatment is the most efficient method to generate various functional groups such as hydroxyl, carbonyl, and carboxylic acid groups on the MWCNT surface.

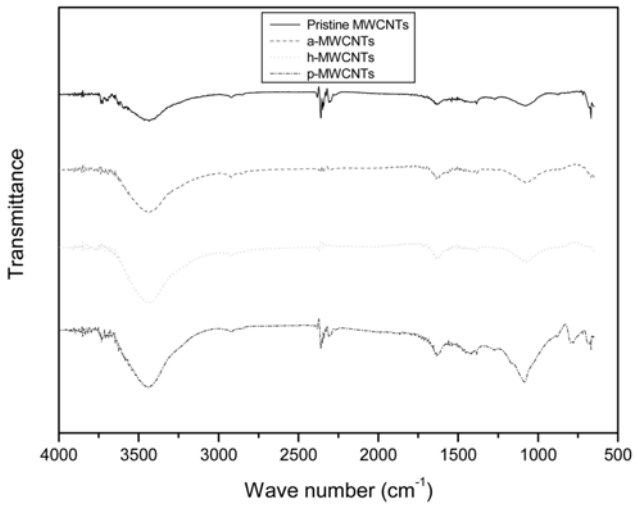

Fig. 2. FT-IR spectra of acid, hot air, and hydrogen peroxide treated MWCNTs.

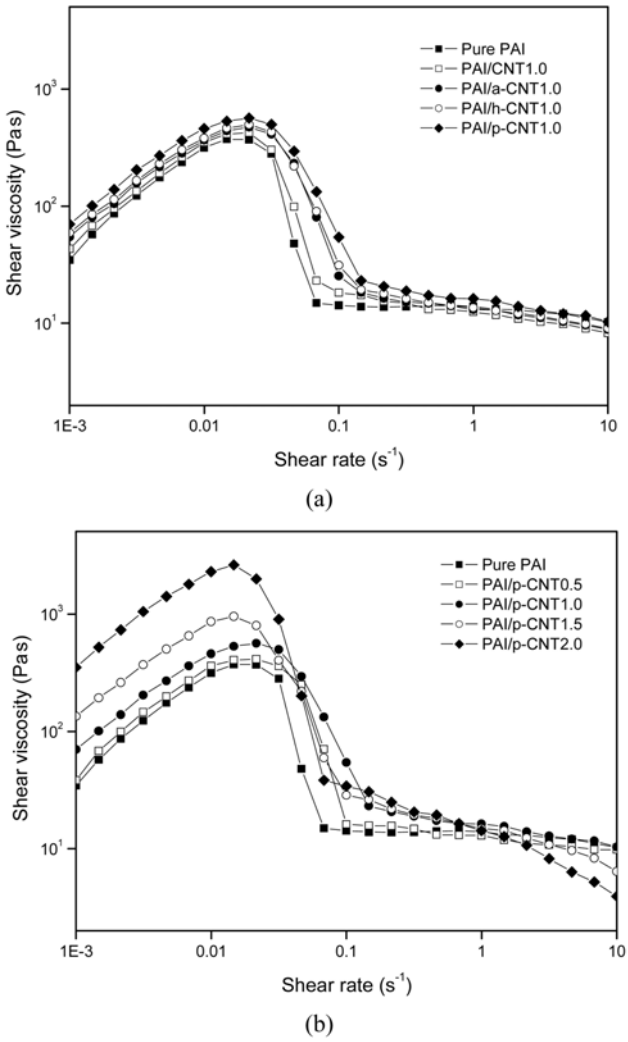

Fig. 3. Effects of (a) chemical functionalization and (b) p-MWCNT contents on the steady shear viscosity of PAI/MWCNT suspensions.

2. Rheological Properties

2-1. Steady Shear Flow Properties

To determine the molecular interaction and dispersion state of MWCNTs in PAI/MWCNT suspensions, rheological properties of pure PAI and PAI/MWCNT suspensions were investigated in both steady and dynamic oscillatory shear flows. As shown in Fig. 3, steady shear viscosity showed the bell-shaped curves with three characteristic ranges: shear thickening at a very low shear rate region (0.001-0.03 s^{-1}), shear thinning at an intermediate shear rate region (0.03-0.1 s^{-1}), and a Newtonian-plateau behavior at a high shear rate region (0.1-10 s^{-1}). The steady shear viscosity of both the pure PAI and PAI/MWCNT suspension was increased abruptly with increasing shear rate and strong shear thickening with a yield stress was observed at a low shear rate region. This unusual behavior reflects that the weak shearing force generated during measurement induces hydrogen bonding or entanglement between PAI molecules as well as PAI molecules and MWCNTs [25-27]. Peng [28] investigated both shear and elongational viscosities for Torlon®4000T-MV and 4000TF solutions to prepare thin hollow membranes for

gas separation. According to the report, 4000T-MV solution showed an overall shear thinning behavior, but the 4000TF solution showed stain hardening due to the strong N-H hydrogen bonding formed in the solutions. Holmes [29] also reported extraordinary rheological behavior of a colloidal suspension showing S-shaped flow curves, indicating shear thickening and stress-induced transitions from a liquid state to a jammed state. As hydrogen bonding was increased, resistance to flow deformation was generally increased in the PAI/NMP solution when sliding and stretching of PAI molecules were present.

After steady shear viscosity passes through maximum values, however, the steady shear viscosity of the pure PAI and PAI/MWCNT suspension was decreased abruptly at the intermediate shear rate range, which reflects that molecular chains are aligned along the shearing flow direction. In general, steady shear viscosity of polymers and polymer/filler composites was decreased gradually with increasing shear rates [30-33]. However, steady shear viscosity of both pure PAI and PAI/MWCNT suspensions was decreased abruptly at short shear rate ranges. The reason is that weak flocculation formed by the hydrogen bonding between PAI molecules as well as functional groups of the PAI resin and MWCNTs was destructed simultaneously at critical shear rate ranges. This exceptional behavior was also reported in liquid crystalline polymer or rod-like molecules, such as poly(*p*-phenyleneterephthalamide) (PPTA), poly(*p*-benzamide), and poly(*p*-phenylenebezobisoxazole) [34-36]. In the case of PPTA in sulfuric acid, steady shear viscosity is increased at a low shear rate range. After the steady shear viscosity reaches a critical value, the viscosity begins to decrease abruptly at short shear rate ranges like the PAI/MWCNT solution investigated in this study. The PPTA molecules remained an isotropic state in the solution with the concentration below the critical value. As soon as the critical concentration was exceeded, however, anisotropic liquid crystalline behavior occurred, resulting in decrease of the solution viscosity.

Effects of chemical functionalization and weight fraction of p-MWCNTs on the steady shear viscosity of the PAI/MWCNT solutions are shown in Figs. 3(a) and (b), respectively. As shown in Fig. 3(a), chemically functionalized MWCNTs/PAI solutions showed increased steady shear viscosity compared with that of the pure PAI solution because strength of hydrogen bonding between PAI precursors and functional groups on MWCNTs was increased. Furthermore, hydrogen peroxide treated MWCNTs/PAI solutions showed the highest steady shear viscosity among chemically functionalized MWCNTs. It is probable that more sites able to form hydrogen bonding with PAI molecules were generated by hydrogen peroxide treatment [7,37]. In Fig. 3(b), effects of p-MWCNT content on the steady shear viscosity of PAI/p-MWCNT solutions were investigated at the concentration ranging from 0.5 to 2.0 wt%. As p-MWCNT content increased in the PAI matrix, the steady shear viscosity increased significantly at a low shear rate region. In general, the yield stress observed at low frequency ranges is generated by hydrogen bonding between chemically functionalized MWCNTs and amide groups in the PAI backbone. At high shear rate regions, however, all specimens have the same value, Newtonian behavior, because they are affected only by the macromolecular chains irrespective of MWCNT content and shear rates. Therefore, the interfacial properties due to hydrogen bonding between PAI molecules and chemically functionalized MWCNTs can affect the rheological properties of the MWCNT-filled suspension. [38].

2-2. Dynamic Oscillatory Shear Flow Properties

It is known that rheological properties measured at a low angular frequency range reflect internal structure of the fluid, e.g., filler dispersion and molecular interaction, whereas rheological properties examined at high shear rates and angular frequency regions reflect processability of polymers and polymer composites [39,40]. Dynamic oscillatory shear flow properties are investigated to elucidate the effects of chemical functionalization and content of MWCNTs on internal structure of PAI/MWCNT composites. Storage modulus and complex viscosity of PAI/MWCNT composites are shown in Figs. 4(a) and (b), respectively. As shown in Fig. 4(a), the highest storage modulus and wide plateau region are observed at low frequency ranges. Like the presence of yield stress in the steady shear flow, the solid-like behavior is generated by the existence of strong hydrogen bonding between PAI molecules and p-MWCNTs [13,41-43]. In Fig. 4(b), complex viscosity has the highest value in the case of PAI/p-MWCNT suspension, which means good dispersion of MWCNTs and strong hydrogen bonding between p-MWCNTs and

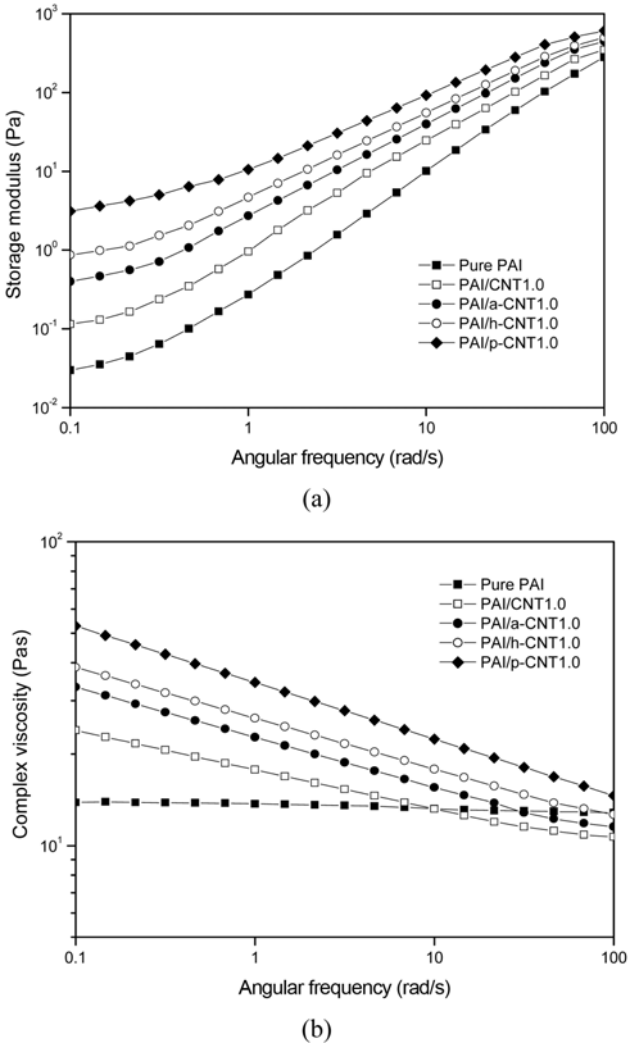

Fig. 4. Effects of chemical functionalization on (a) storage modulus and (b) complex viscosity of PAI/MWCNT1.0 suspensions.

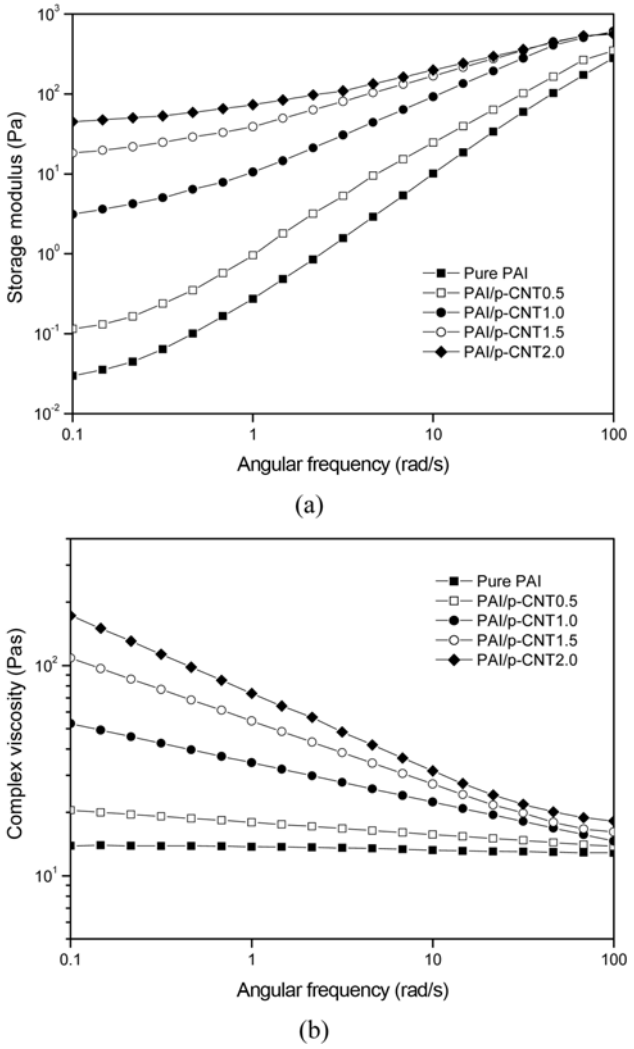

Fig. 5. Effects of p-MWCNT content on (a) storage modulus and (b) complex viscosity of PAI/p-MWCNT suspensions.

PAI molecular chains due to effective chemical functionalization of the p-MWCNT surface. The PAI suspensions filled with surface-modified MWCNTs have higher storage modulus and complex viscosity than pristine MWCNTs/PAI composites since the interaction force between MWCNTs and PAI molecules becomes larger. Especially, PAI/p-MWCNT suspension shows the highest storage modulus and complex viscosity due to good dispersion and strong hydrogen bonding formed between PAI molecules and p-MWCNTs.

In Figs. 5(a) and (b), effects of p-MWCNT content on storage modulus and complex viscosity of PAI/p-MWCNT suspensions are illustrated as a function of angular frequency. Maximum complex viscosity of the PAI/p-MWCNT suspension at low frequency range was increased with increasing p-MWCNT content as shown in Fig. 5(a). In general, molecular interaction between MWCNTs is increased as the MWCNT content is increased in polymer matrix. Storage modulus and complex viscosity are increased significantly when the MWCNT content is increased from 0.5 to 1.0 wt%, which means that a change from liquid-like to solid-like behavior occurs in the PAI/p-MWCNT suspension. In the PAI/p-MWCNT suspensions filled with p-MWCNTs of 1.5 and 2.0 wt%, however, it is not easy to confirm that interaction between p-MWCNTs and PAI molecules is increased with increasing p-MWCNT content. Molecular interaction and hydrogen bonding between MWCNTs and functional groups of the PAI molecules are not increased linearly with respect to the weight fraction of the MWCNTs, as shown by the experimental results obtained through dynamic oscillatory flow measurement [44,45].

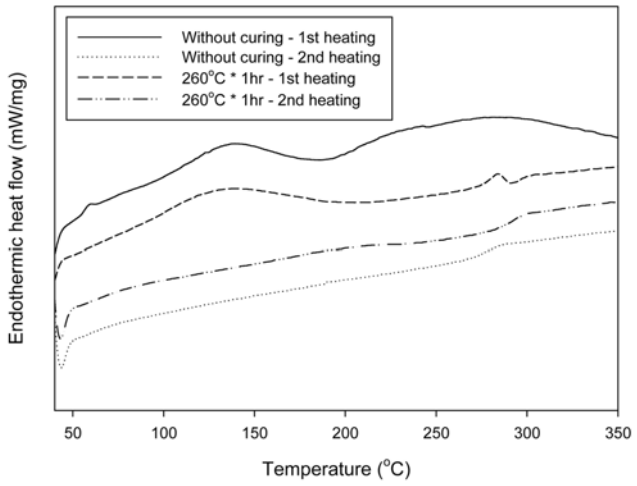

Fig. 6. The first and second heating DSC thermograms of pure PAI films treated with or without thermal curing.

2-3. Thermal Curing Behavior

The PAI resin maintains remarkable mechanical properties and thermal stability at high temperature due to high T_g which is above 270 °C. Therefore, glass transition behavior and thermal curing of the PAI resin are essential to understand the thermal stability and mechanical properties of the final PAI product. In this study, effects of chemical functionalization and weight fraction of MWCNTs on T_g and thermal curing time of PAI/MWCNT composites were investigated with DSC measurement. Fig. 6 shows the first and second heating curves of the pure PAI films with or without thermal curing. As shown, DSC characteristic peaks are observed at near 150 °C from the first heating curves, which implies that the solvent is not removed completely in PAI/NMP suspensions. From the second heating curves the T_g of the pure PAI film is in the range of 260-270 °C, indicating the high stiffness characteristics of the PAI molecular chains at high temperature [46,47]. Especially, the PAI film cured at 280 °C for 1 hour shows higher T_g when compared with that of the pure PAI film without thermal curing. The difference in T_g values of the pure PAI films may be attributed to the presence of rigid aromatic and heterocyclic structures with compact imide ring units formed by thermal imidization.

Effects of curing time on T_g of the pure PAI and PAI/p-MWCNT1.0 composite films are shown in Figs. 7(a) and (b), respectively. As shown in Fig. 7(a), the pure PAI film without thermal curing shows T_g approximately at 272 °C but does not have a distinct inflection point showing glass-rubber transition behavior. However, T_g of the pure PAI films was increased significantly as the curing time was increased from 6 to 18 hours because a more perfect heterocyclization reaction occurred along the PAI molecular backbone and molecular weight was increased by dehydration reaction during thermal curing [48]. Effects of thermal curing time on T_g of the PAI/p-MWCNT1.0

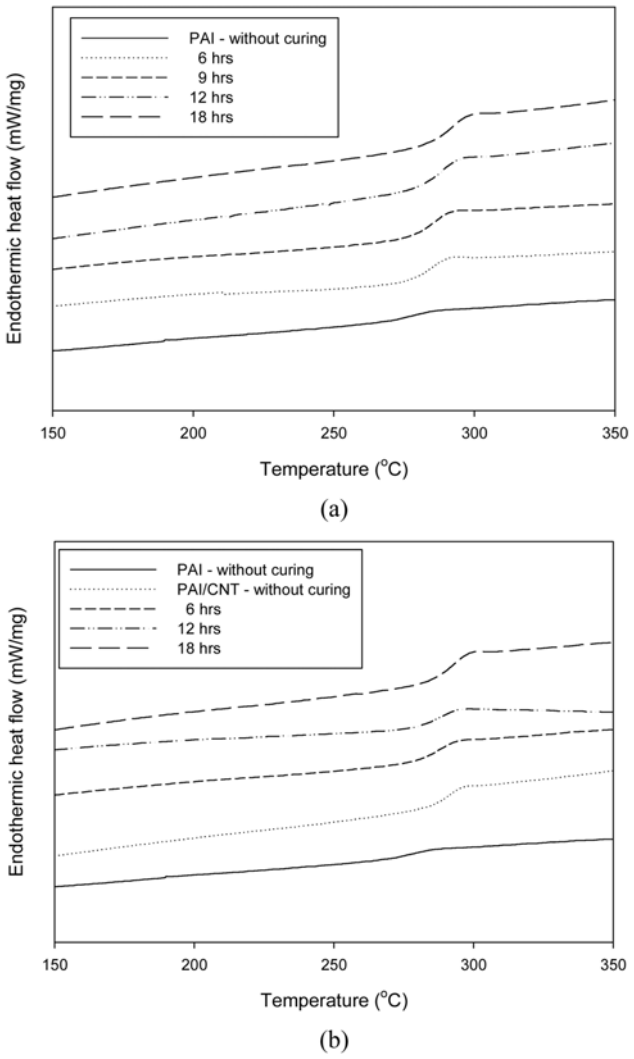

Fig. 7. The second heating DSC thermograms showing effects of thermal curing time on T_g of (a) pure PAI and (b) PAI/p-MWCNT1.0 composite films.

composite films are shown in Fig. 7(b). T_g of the PAI/p-MWCNT1.0 composite films was also increased with increasing thermal curing time from 6 to 18 hours like the pure PAI film. However, when they were cured for the same time, PAI/p-MWCNT1.0 composite films had higher T_g than the pure PAI film because the molecular chains are confined between the reinforcing fillers with different dispersion states. T_g is related to the confinements introduced by finite pores and pressure effects of constraints generated during fabrication of polymeric composites [49].

Effects of the p-MWCNT content on T_g of the PAI/p-MWCNT composite films are shown in Fig. 8. By incorporating p-MWCNTs of 0.5 wt% into the PAI matrix, T_g of the PAI/p-MWCNT composite was increased when compared with that of the pure PAI film. As the p-MWCNT content was increased more, T_g higher than that of the PAI film was also observed. Since T_g is the characteristic temperature corresponding to segmental motion of polymer chains at the molecular level, T_g can be considered as one of the localized phenomena for polymers and polymer composite systems [50]. Therefore, it was found that MWCNTs with high stiffness act as con-

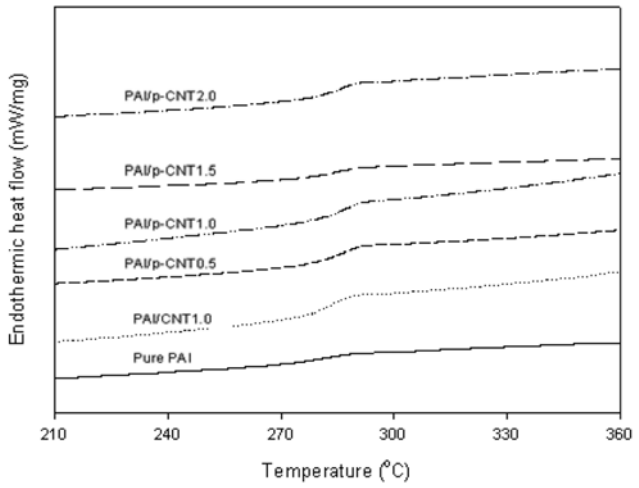

Fig. 8. The second heating DSC thermograms showing effects of p-MWCNT content on T_g of PAI/p-MWCNT composite films cured at 260 °C for 12 hours.

finement to polymer chains at the molecular level and obstruct the localized segmental motions of PAI chains, resulting in the increase of T_g from 280 °C to around 300 °C. Consequently, the mobility of PAI molecules is reduced when sufficient molecular constraints exist on PAI chains, leading to an increase in T_g [51-53]. Although T_g was increased by further incorporation of p-MWCNTs, plateau values of T_g were observed with the p-MWCNT contents of 1.5 to 2.0 wt%. When weight fraction of the p-MWCNTs is over 1.5 wt%, PAI molecular chains have the almost similar mobility level, leading to relatively smaller change in T_g than the PAI molecular chains. It is concluded that the T_g values of PAI/p-MWCNT composites were increased with increasing p-MWCNT content and curing time. However, selection of the optimum MWCNT content is essential to improve physical properties of PAI/MWCNT composites since many other properties, e.g., melt viscosity and processability are determined by the dispersion state of MWCNTs.

CONCLUSIONS

PAI/MWCNT composites were prepared by using solution mixing with ultrasonic excitation to investigate effects of surface modification and weight fraction of MWCNTs on rheological properties and thermal curing behavior of PAI/MWCNT composite films. Steady shear viscosity curves showed the bell-shaped patterns with three characteristic ranges: shear thickening, shear thinning, and nearly Newtonian plateau behavior. They also showed higher storage modulus and complex viscosity than the pure PAI resin because molecular interactions between functionalized MWCNTs as well as MWCNTs and functional groups in the PAI resin were increased. Especially, p-MWCNTs/PAI composites exhibited the highest storage modulus and complex viscosity. Glass transition temperature of the pure PAI and PAI/MWCNT composite film was increased significantly with increasing curing time because perfect heterocyclic structure is formed along the molecular backbone and molecular weight is increased by dehydration and crosslinking reaction during thermal curing. When p-MWCNT content is over 1.5 wt%, molecular chains have an almost similar mobility level, leading to a relatively smaller

change in T_g compared with the PAI resin. It was concluded that T_g of the pure PAI or the PAI/MWCNT composite film was increased with increasing MWCNT content and thermal curing time. However, it is essential to consider optimum MWCNT content and thermal curing conditions since many physical properties of the PAI/MWCNT composite films are determined by both weight fraction and dispersion of MWCNTs in the PAI matrix.

ACKNOWLEDGMENTS

This study was supported by the Korea Science and Engineering Foundation (KOSEF) grant funded by the Korean government (MEST) (R11-2005-065) through the Intelligent Textile System Research Center (ITRC).

REFERENCES

1. J. M. Margolis, *Engineering plastics handbook*, McGraw-Hill, New York (2006).
2. S. Mehdipour-Ataei and M. Hatami, *Eur. Polym. J.*, **41**, 2010 (2005).
3. G. P. Robertson, M. D. Guiver, M. Yoshikawa and S. Brownstein, *Polymer*, **45**, 1111 (2004).
4. Y. Wang, S. H. Goh and T. S. Chung, *Polymer*, **48**, 2901 (2007).
5. D. J. Liaw, F. C. Chang, J. H. Liu, K. L. Wang, K. Faghihi and S. H. Huang, *Polym. Degrad. Stab.*, **92**, 323 (2007).
6. P. Liu, *Eur. Polym. J.*, **41**, 2693 (2005).
7. Y. T. Sung, M. S. Han, K. H. Song, J. W. Jung, H. S. Lee, C. K. Kum, J. Joo and W. N. Kim, *Polymer*, **47**, 4434 (2007).
8. V. Datsyuk, P. Landois, J. Fitremann, A. Peigney, A. M. Galibert, B. Soula and E. Flahaut, *J. Mater. Chem.*, **19**, 2729 (2009).
9. S. H. Lee, M. W. Kim, S. H. Kim and J. R. Youn, *Eur. Polym. J.*, **44**, 1620 (2008).
10. J. A. Kim, D. G. Seong, T. J. Kang and J. R. Youn, *Carbon*, **44**, 1898 (2006).
11. C. Gao, H. He, L. Zhou, X. Zheng and Y. Zhang, *Chem. Mater.*, **21**, 360 (2009).
12. K. Yang, M. Gu, Y. Guo, X. Pan and G. Mu, *Carbon*, **47**, 1723 (2009).
13. S. H. Lee, E. Cho, S. H. Jeon and J. R. Youn, *Carbon*, **45**, 2810 (2007).
14. M. Kang, *Korean J. Chem. Eng.*, **25**, 933 (2008).
15. C. P. Yang, R. S. Chen and C. S. Wei, *Eur. Polym. J.*, **38**, 1721 (2002).
16. H. Behniafar and S. Haghighat, *Eur. Polym. J.*, **42**, 3236 (2006).
17. A. Ranade, N. A. D'Souza and B. Gnade, *Polymer*, **43**, 3759 (2002).
18. L. Shi, Y. Zhao, X. Zhang, H. Su and T. Tan, *Korean J. Chem. Eng.*, **25**, 1434 (2009).
19. P. R. Buch, D. J. Mohan and A. V. R. Reddy, *Polym. Int.*, **55**, 391 (2006).
20. D. Ratna, T. Abraham and J. Karger-Kocsis, *Macromol. Chem. Phys.*, **209**, 723 (2008).
21. T. N. Abraham, D. Ratna, S. Siengchin and J. Karger-Kocsis, *J. Appl. Polym. Sci.*, **110**, 2094 (2008).
22. J. R. Vail, D. L. Burris and W. G. Sawyer, *Wear*, **267**, 619 (2009).
23. Solvay Advanced Polymers Data Sheet. http://www.solvayadvancedpolymers.com.
24. Carbon nano-material technology data sheet. http://www.carbonnano.co.kr/english/english.htm.
25. R. G. Larson, *The structure and rheology of complex fluids*, Oxford University Press, New York (1999).
26. J. M. Dealy and K. F. Wissbrun, *Melt rheology and its role in plastics processing*, Van Nostrand Reinhold, New York (1990).
27. S. H. Lee, J. H. Kim, S. H. Choi, S. Y. Kim, K. W. Kim and J. R. Youn, *Polym. Int.*, **58**, 354 (2009).
28. N. Peng, T. S. Chung and J. Y. Lai, *J. Membrane. Sci.*, **326**, 608 (2009).
29. C. B. Holmes, M. E. Cates, M. Fuchs and P. Sollich, *J. Rheol.*, **49**, 237 (2005).
30. A. V. Shenoy, *Rheology of filled polymer systems*, Kluwer Academic Publisher, Dordrecht (1999).
31. R. K. Gupta, *Polymer and composite rheology*, Marcel Dekker, New York (2000).
32. E. Brown and H. M. Jaeger, *Phys. Rev. Lett.*, **103**, 086001 (2009).
33. R. Olejnik, P. Liu, P. Slobodian, M. Zatloukal and P. Saha, *AIP Conf. Proc.*, **1152**, 204 (2009).
34. D. R. Salem, *Structure formation in polymeric fibers*, Hanser Publishers, Munich (2001).
35. P. W. Morgan, *Macromolecules*, **10**, 1381 (1977).
36. E. W. Choe and S. N. Kim, *Macromolecules*, **14**, 920 (1981).
37. S. I. Cha, K. T. Kim, K. H. Lee, C. B. Mo, Y. J. Jeong and S. H. Hong, *Carbon*, **46**, 482 (2008).
38. K. Q. Xiao, L. C. Zhang and I. Zarudi, *Compos. Sci. Technol.*, **67**, 177 (2007).
39. P. Pötschke, T. D. Fornes and D. R. Paul, *Polymer*, **43**, 3247 (2002).
40. L. Chen, X. J. Pang and Z. L. Yu, *Mater. Sci. Eng.*, **457**, 287 (2007).
41. A. T. Seyhan, F. H. Gojny, M. Tanoğlu and K. Schulte, *Eur. Polym. J.*, **43**, 2836 (2007).
42. Z. Fan and S. G. Advani, *J. Rheol.*, **51**, 585 (2007).
43. S. H. Lee, E. Cho and J. R. Youn, *J. Appl. Polym. Sci.*, **103**, 3506 (2007).
44. H. Yang, B. Li, K. Wang, T. Sun, X. Wang, Q. Zhang, Q. Fu, X. Dong and C. C. Han, *Eur. Polym. J.*, **44**, 113 (2008).
45. S. H. Lee, J. S. Park, B. K. Lim and S. O. Kim, *J. Appl. Polym. Sci.*, **110**, 2345 (2008).
46. T. Hatakeyama and F. X. Quinn, *Thermal analysis: Fundamentals and applications to polymer science*, John Wiley & Sons, New York (1999).
47. M. K. Ghosh and K. L. Mittal, *Polyimide: Fundamentals and applications*, Marcel Dekker, New York (1996).
48. K. C. Chan and T. C. Chang, *Polym. J.*, **30**, 897 (1998).
49. H. Cai, F. Yan and Q. Xue, *Mater. Sci. Eng. A*, **364**, 94 (2004).
50. K. P. Menard, *Dynamic mechanical analysis: A practical introduction*, CRC Press, Boca Raton, FL (1999).
51. K. S. Kang, S. I. Lee, T. J. Lee, R. Narayan and B. Y. Shin, *Korean J. Chem. Eng.*, **25**, 599 (2008).
52. Q. P. Feng, X. M. Xie, Y. T. Liu, W. Zhao and Y. F. Gao, *J. Appl. Polym. Sci.*, **106**, 2413 (2007).
53. B. Vigolo, V. Mamane, F. Valsaque, T. N. H. Le, J. Thabit, J. Ghanbaja, L. Aranda, Y. Fort and E. McRaea, *Carbon*, **47**, 411 (2009).